



Design of a bio-inspired imidazole-based iron catalyst for epoxidation of olefins: Mechanistic insights

Kristin Schröder, Kathrin Junge, Anke Spannenberg, Matthias Beller*

Leibniz-Institut für Katalyse e.V. an der Universität Rostock, Albert-Einstein-Str. 29a, D-18059 Rostock, Germany

ARTICLE INFO

Article history:

Available online 9 June 2010

Keywords:

Epoxidation
Iron
Homogeneous catalysis
Hydrogen peroxide
N-ligands

ABSTRACT

A novel defined iron catalyst for the epoxidation of aromatic and aliphatic olefins with hydrogen peroxide as the terminal oxidant is described. Our catalyst approach is based on bio-inspired both alkyl- and aryl-substituted imidazoles in combination with cheap and abundant iron trichloride hexahydrate. Heterocycles similar to imidazole can be used as ligands in this epoxidation system, too. The novel system is stable towards air and water. It is shown that the mechanism depends strongly on the used ligands and substrates. In the presence of radical scavengers no carbon-centered radical could be detected.

© 2010 Elsevier B.V. All rights reserved.

1. Introduction

The catalytic epoxidation of olefins providing oxiranes constitutes an important and challenging oxidation reaction. From an industrial point of view aliphatic epoxides are of special interest, namely 1,2-propylene oxide and ethylene oxide, which are annually produced on a million ton-scale [1]. State-of-the-art heterogeneous catalysts like Ti-substituted silicalite (TS-1) for the epoxidation of propylene [2] or supported silver catalysts on Al_2O_3 for the production of ethylene oxide [3] make use of benign oxidants such as hydrogen peroxide or molecular oxygen. Clearly, these heterogeneous catalysts have advantages with respect to separation and reuse. Nevertheless, in general they require relatively harsh reaction conditions and are more difficult to mechanistically understand on a molecular basis [4]. Hence, there is a continuing interest in active, selective and molecular-defined epoxidation catalysts. In this respect transition metal complexes provide powerful and tunable models for new type of oxidation catalysts. Homogeneous metal complexes which provide active epoxidation catalysts in the presence of hydrogen peroxide are mainly based on ruthenium [5], rhenium [6], manganese [7], and in the recent past iron [8]. Notably, until today the development of a general applicable, active and selective catalyst system which is able to epoxidize both aromatic and aliphatic olefins is still a challenging goal.

Iron-based catalysts offer significant advantages compared to precious metals like abundance and low toxicity [9]. Obviously, a variety of iron salts and iron complexes are commercially available

on a large scale. Moreover, it is noteworthy that iron is involved in manifold biological systems, for instance in metalloproteinase like methane monooxygenases as diiron core for the metabolic aerobic pathway of methane to methanol [10]. Based on these structurally well-characterized enzymes, model complexes have been prepared to explore mainly mechanistic issues and partially oxidation catalysis. Unfortunately, most of the known systems have limitations including tedious complex preparation, limited substrate scope, low selectivity and/or the use of 'non-green' and expensive oxidants such as hypervalent iodo compounds, peracids etc. [11].

Recently, we demonstrated the conversion of various olefins to the corresponding epoxides using hydrogen peroxide in the presence of an in situ generated catalyst composed of $\text{FeCl}_3 \cdot 6\text{H}_2\text{O}$, pyridine-2,6-dicarboxylic acid (H_2pydic), and an organic base like pyrrolidine, *N*-benzylamines or formamides [12–14]. Unfortunately, these in situ generated catalysts are difficult to study mechanistically. Therefore, we designed a bio-inspired two-component-protocol consisting of imidazole derivatives as ligands and iron as catalyst core [15]. Here, we report an account of our work on iron–imidazole systems and additional novel mechanistic insights.

2. Experimental

2.1. General remarks

The imidazole ligands **12** and **13** were synthesized according to a known literature protocols [16]. All other reagents were used as purchased from commercial suppliers (Aldrich, Fluka, Merck, etc.) without further purification. "30%" aqueous H_2O_2 from Merck was used as received. The peroxide content varied from 30% to 40%

* Corresponding author. Tel.: +49 381 1281113; fax: +49 381 12815113.
E-mail address: matthias.beller@catalysis.de (M. Beller).

as determined by titration. GC analyses were performed with a Hewlett Packard HP 6890. GC calibrations for alkenes and epoxides were carried out with authentic samples and dodecane as an internal standard. Mass spectra were in general recorded on a HP 5989A EI mass selective detector. NMR spectra were measured using a Bruker ARX 300 or ARX 400 spectrometer.

2.2. General procedure for the epoxidation of olefins

In a test tube, $\text{FeCl}_3 \cdot 6\text{H}_2\text{O}$ (0.025 mmol), *t*-amyl alcohol (9 mL), heterocyclic ligand (0.05 mmol), olefin (0.5 mmol) and dodecane (GC internal standard, 100 μL) were added in sequence at room temperature in air. To this stirred mixture a solution of 30% hydrogen peroxide (aqueous, 170 μL , 1.5 mmol) in *t*-amyl alcohol (830 μL) was added over a period of 1 h at room temperature by a syringe pump. Conversion and yield were determined by GC analysis without further manipulations and compared with authentic samples.

2.3. X-ray data

Data were collected on a STOE IPDS II diffractometer using graphite-monochromated Mo $K\alpha$ radiation. The structures were solved by direct methods (SHELXS-97) [17] and refined by full-matrix least-squares techniques on F^2 (SHELXL-97) [18]. XP (Bruker AXS) was used for graphical representations. CCDC 748745 contains the supplementary crystallographic data for (*mer*-[Fe^{III} (**13**) Cl_3]) in this paper. CCDC 714375–714377 contain additional data for complexes *trans*-[$\text{FeCl}_2(\mathbf{2})_4$] Cl and [(**12**) $_4$ ClFeOFeCl_3] [15b]. These data can be obtained free of charge from The Cambridge Crystallographic Data Centre via www.ccdc.cam.ac.uk/data_request/cif.

3. Results and discussion

3.1. Catalysis results

The starting point of our work was inspired by a closer look to known oxidatively active enzymes. In the majority of these enzymes with an iron core a similar structural motif of ligands surrounding the metal inside the enzyme is found [19]. Next to amino acid residues like aspartate, glutarate or cysteine and co-factors like α -ketoglutarate in non-heme enzymes, histidine ligands are involved in nearly all enzymes whereas histidine displaces one of the essential amino acids. The imidazole scaffold binds mainly to the iron center in non-heme enzymes (Fig. 1) [20].

In Table 1 the reactivities of different imidazoles and additional heterocycles are shown. As a typical benchmark reaction the epoxidation of *trans*-stilbene in the presence of $\text{FeCl}_3 \cdot 6\text{H}_2\text{O}$ and 30% H_2O_2 as terminal oxidant was investigated.

The previously best performing co-ligand pyrrolidine (Table 1, entry 1) did not show any activity without H_2pydic . $\text{FeCl}_3 \cdot 6\text{H}_2\text{O}$ itself without any ligands showed a certain activity in the presence of hydrogen peroxide (blank sample: 5% yield with 31% selectivity for *trans*-stilbene). Simple imidazole **3** gave the corresponding oxirane in 38% yield with a selectivity of 90% (Table 1, entry 3). Other basic heterocyclic ligands such as pyrazole **4** gave similar yields but slightly higher conversion (Table 1, entry 4). Both methylated heterocycles showed diminished yield at high selectivity compared to their non-methylated counterparts (Table 1, entries 8 and 9), whereas imidazole **8** gave significantly higher yield than pyrazole **9**. Aryl-substituted derivatives show even more pronounced effects: while phenyl-imidazole **10** provided good yields phenylpyrazole **11** showed nearly no yield. Even though imidazole and pyrazole are similar, in general electronically there are some differences. Besides, the free 2-position at the imidazole scaffold is

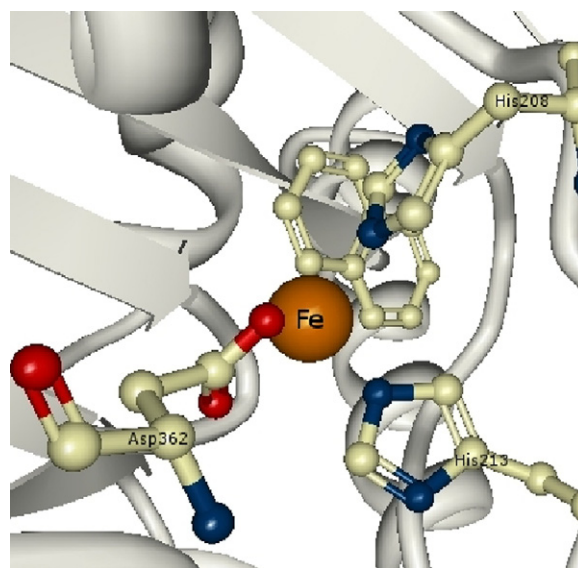


Fig. 1. Naphthalene dioxygenase with a mononuclear iron at the active site [20].

of importance for the stabilizing hydrogen bonding in the epoxidation reaction as previously discussed [15b]. By changing the pyrrole nitrogen of the imidazole towards oxygen or sulphur (Table 1, entries 3, 6 and 7) a drop in activity was observed in each case. The best performances were still shown with imidazoles **2** and **12**; an overview is presented in Scheme 1 [15].

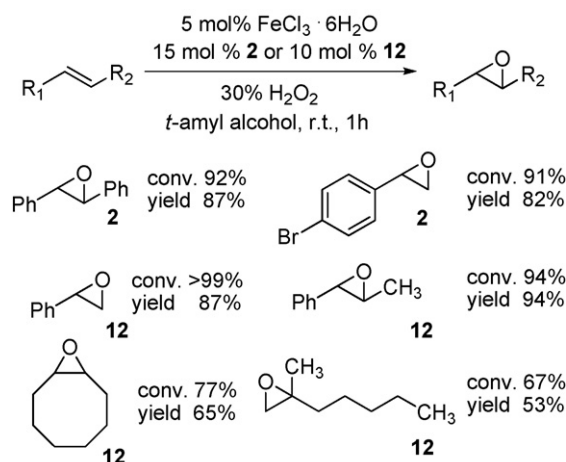
Stilbenes and styrenes were epoxidized with ligand **2** in high yields with good selectivity. Additional various aliphatic olefins showed with imidazole **12** significant higher yields, e.g. cyclooctene was oxidized in up to 65% yield with 84% selectivity.

3.2. Mechanistic investigations

In Scheme 2 we proposed a mechanism for the epoxidation of olefins in the presence of a dimeric and a monomeric iron imidazole complex, based on our previous results [15].

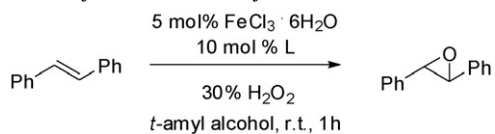
A competitive equilibrium between the μ -oxo diiron complexes **A** and the more active mononuclear $\text{Fe}(\text{III})$ -complex **B** by reaction with water was adopted [21]. Apparently, **A** is easily converted to the active species. After ligand solvent exchange **C** the resulting hydroperoxo complex **D** is stabilized intramolecularly by hydrogen bonding from the attached ligand.

In order to elucidate the mechanism in more detail, here we report on the influence of ligands on the reactivity of the iron cen-



Scheme 1. Selection of obtained yields of various olefins.

Table 1
Reactivity of different heterocycles in the benchmark reaction^a



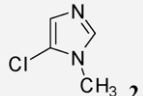
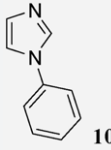
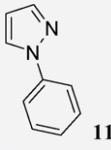
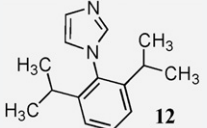
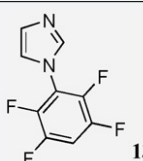
No	Ligand (L)	Conv. [%] ^b	Yield [%] ^b	Sel. [%] ^c
1	 1	4	2	40
2	 2	83	80	97
3	 3	43	38	90
4	 4	53	42	79
5	 5	36	30	83
6	 6	34	18	54
7	 7	30	29	98
8	 8	19	18	91
9	 9	7	6	82
10	 10	74	66	89
11	 11	8	2	32
12	 12	72	66	92

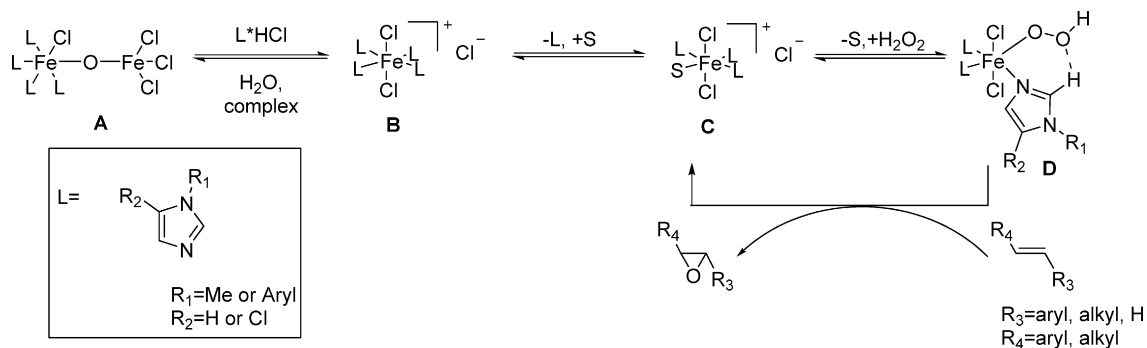
Table 1 (Continued)

No	Ligand (L)	Conv. [%] ^b	Yield [%] ^b	Sel. [%] ^c
13		76	70	92

^a Reaction conditions: in a test tube, FeCl₃·6H₂O (0.025 mmol), heterocyclic derivative (0.05–0.075 mmol), *tert*-amyl alcohol (9 mL), *trans*-stilbene (0.5 mmol) and dodecane (GC internal standard, 100 μL) were added in sequence at r.t. in air. To this mixture, a solution of 30% H₂O₂ (170 μL, 1.5 mmol) in *tert*-amyl alcohol (830 μL) was added over a period of 1 h at r.t. by a syringe pump.

^b Conversion and yield were determined by GC analysis.

^c Selectivity refers to the ratio of yield to conversion in percentage.



Scheme 2. Proposed mechanism of the epoxidation reaction with the iron/imidazole system [15b].

ter. In addition, the formation of radicals and the influence of air and water were studied. In order to get an indication of the occurrence of radicals, β-pinene was applied as substrate in the presence of the best two ligands **2** (from the alkyl-substituted imidazoles) and **12** (from the 1-aryl-substituted imidazoles). It should be noted that β-pinene points to the formation of radical intermediates via rearrangement of the tensed four-membered carbon cycle (Fig. 2) [22].

Surprisingly, the obtained results varied significantly depending on the ligand. With 91% conversion the main product of the epoxidation of β-pinene with ligand **12** was the corresponding epoxide **14a**. Next to allylic oxidation product **14b** which was detected in small amounts, also traces of cleavage product nopinone **14c** were detected by GC–MS analysis (pathway A). Perillyl alcohol **14e** and hydroxylated derivatives **14d** (and analogues), which indicated the

formation of OH• radicals (pathway B) were only observed in small traces similar to **14c**. Ligand **2** gave entirely different results. Instead of any epoxide formation, the oxidation gave no main product with 54% conversion of the olefin. Next to **14b** and traces of **14c** also the rearrangement products **14d** and **14e** were observed both in similar small quantities than **14b**. In contrast to the epoxidation reaction with ligand **12** application of ligand **2** leads to a less active and also OH• radical-based reaction. However, aromatic olefins gave 40% yield or more of the corresponding oxiranes and high selectivities (>85%) using ligand **2** [15a]. These results clearly demonstrate the strong influence of the ligand depending on the substrate.

Next, three radical scavengers were applied to see further effects (Fig. 3). Applying our benchmark system with ligands **2**, **12** and also **4** in the presence of duroquinone (2,3,5,6-tetramethyl-*p*-benzoquinone) (1 equiv. and 5 mol%) no change in yield or conversion was observed. This shows that duroquinone neither plays a role as ligand [23] nor is involved in radical inhibition [24].

A different behavior was observed in the presence of TEMPO (2,2,6,6-tetramethylpiperidine-1-oxyl) and BPN (*N*-*tert*-

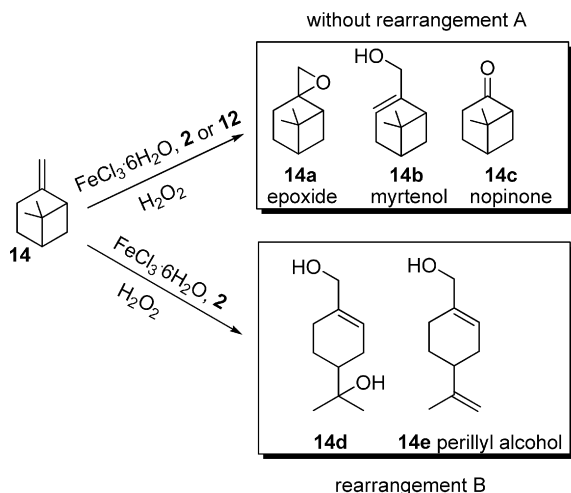


Fig. 2. Products during the oxidation of β-pinene.

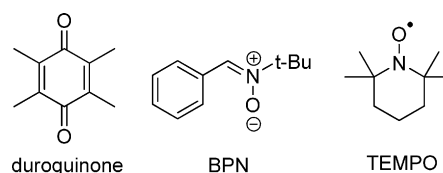


Fig. 3. Radical scavengers applied in the iron/imidazole catalyzed epoxidation reaction.

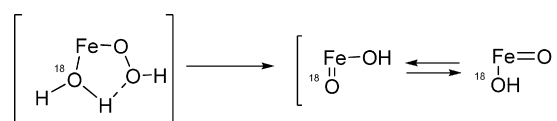
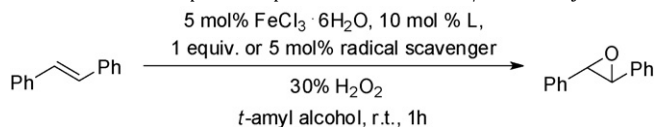


Fig. 4. Proposed oxo-hydroxo tautomerism.

Table 2
Behavior of radical traps in the epoxidation with the iron/imidazole system^a



No.	Radical scavenger [mmol]	Ligand	Conv. [%] ^b	Yield [%] ^b	Sel. [%] ^c
1	–	12	72	66	92
2	–	2	83	80	97
3	BPN [0.5]	12	55 (61) ^d	44 (51) ^d	80 (83) ^d
4	BPN [0.025]	12	67	62	93
5	BPN [0.5]	2	64 (64) ^d	52 (55) ^d	82 (87) ^d
6	BPN [0.025]	2	84	74	88
7	TEMPO [0.5]	12	1	1	94
8	TEMPO [0.025]	12	23	18	78
9	TEMPO [0.5]	2	6	5	84
10	TEMPO [0.025]	2	62	45	73

^a Reaction conditions: in a test tube, FeCl₃·6H₂O (0.025 mmol), imidazole derivative (0.05 mmol), *tert*-amyl alcohol (9 mL), *trans*-stilbene (0.5 mmol) and dodecane (GC internal standard, 100 μL) were added in sequence at r.t. in air. The radical scavenger (1 equiv. or 5 mol%) was added directly before the H₂O₂ addition or with a delay of 15 min. To this mixture, a solution of 30% H₂O₂ (170 μL, 1.5 mmol) in *tert*-amyl alcohol (830 μL) was added over a period of 1 h at r.t. by a syringe pump.

^b Conversion and yield were determined by GC analysis.

^c Selectivity refers to the ratio of yield to conversion in percentage.

^d The radical trap was added to the solution with delay of 15 min after the addition of hydrogen peroxide.

butylphenylnitron) as radical scavengers, which should trap possible existing carbon-centered radicals. Employing BPN in the benchmark reaction for ligands **2** and **12** slightly decreased yields and conversions were observed (Table 2, entries 3–6). However,

no carbon-centered radical was noticed by direct addition. Slow addition of the radical trap BPN gave a high yield of benzaldehyde (69% for entry 3), which mainly arose by the decomposition of the nitron trap. Therefore the possible amount of benzaldehyde

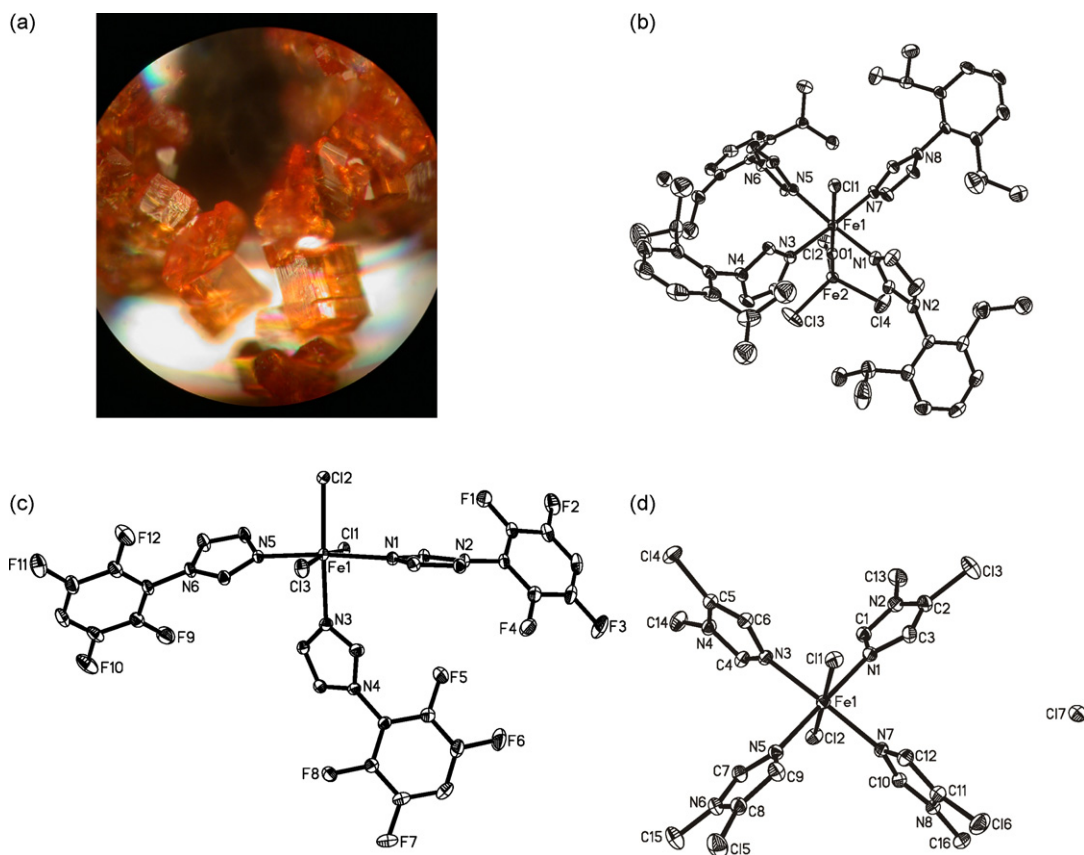
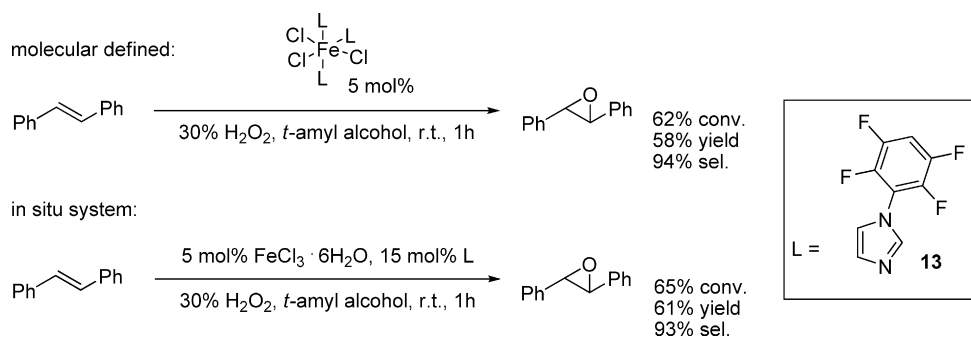


Fig. 5. Three different types of involved iron complexes (hydrogen atoms are omitted for clarity): (a) crystals of the complex Fe(**12**)₄Cl–O–FeCl₃. Selected bond distances (Å) and angles (°): Cl1–Fe1 2.4548(8), Cl2–Fe2 2.2309(9), Fe1–O1 1.8184(19), Fe1–N7 2.128(2), Fe1–N5 2.136(2), Fe1–N1 2.138(2), Fe1–N3 2.151(2), Fe2–O1 1.7651(18); O1–Fe1–N7 92.64(8), N7–Fe1–N5 89.67(8), N5–Fe1–N1 174.17(9), N7–Fe1–N3 175.56(9), O1–Fe1–Cl1 178.20(6), O1–Fe2–Cl3 110.86(7), Cl3–Fe2–Cl4 107.45(5). (b) ORTEP diagram of the corresponding crystal structure. Selected bond distances (Å) and angles (°): Cl1–Fe1 2.3777(6), Cl2–Fe1 2.3096(5), Cl3–Fe1 2.3071(6), Fe1–N5 2.1319(15), Fe1–N1 2.1524(15), Fe1–N3 2.1684(16); N5–Fe1–N1 174.18(6), N5–Fe1–N3 87.86(6), N5–Fe1–Cl3 91.61(5), N1–Fe1–Cl3 90.62(5), N3–Fe1–Cl2 175.13(5), Cl3–Fe1–Cl2 96.10(2), Cl3–Fe1–Cl1 173.44(2). (c) ORTEP diagram of Fe(**13**)₃Cl₃, and (d) ORTEP diagram of *trans*-[FeCl₂(**2**)₄]Cl. The thermal ellipsoids correspond to 30% probability. Selected bond distances (Å) and angles (°): N1–Fe1 2.123(2), N3–Fe1 2.1315(19), N5–Fe1 2.125(2), N7–Fe1 2.1518(19), Cl1–Fe1 2.3115(6), Cl2–Fe1 2.3036(7); N1–Fe1–N5 177.58(8), N1–Fe1–N3 90.57(8), N1–Fe1–Cl2 89.99(6), Cl2–Fe1–Cl1 176.77(3).



Scheme 3. Comparison of the molecular-defined catalyst with the in situ system under our reaction conditions.

in these reactions is enhanced; it displays not only the byproduct but also the decomposition product. Furthermore, *cis*-cyclooctene was used as substrate. As expected ligand **12** gave significantly higher yield (37% yield with 76% selectivity) compared to ligand **2** (13% yield with 58% selectivity) in the presence of 0.5 mmol BPN. Although ligand **2** yielded less epoxide the decomposition of the nitron trap to benzaldehyde was almost complete. In the case of ligand **12** the nitron trap as well as **12** was still observable in GC-MS.

When TEMPO was applied as an additive it mainly inhibited the epoxide formation, whereas no trapped species could be detected. Contrary to known alcohol oxidations the persistent TEMPO radical does not favor the oxidation process [25]. In no case carbon-centered radical could be observed.

Next, the role of water was confirmed. This is of special interest due to the possible exchange between the oxygen of the hydroperoxide and of the water via tautomeric iron-oxo species (Fig. 4) [26]. A competitive equilibrium was proposed between less active μ -oxo diiron complexes (Scheme 2, A) and the active mononuclear Fe(III)-complex (Scheme 2, B) by reaction with water. Preliminary investigations of the epoxidation of *trans*-stilbene with ligands **2** and **12** in the presence of 10 equiv. of water and 50% H_2O_2 or the urea- H_2O_2 adduct as oxidant again showed the striking influence of the ligand. Low conversion and yield were observed with ligand **12**. However, in the presence of ligand **2** and 50% hydrogen peroxide as oxidant 36% conversion with 35% yield was obtained after 1 h addition. The yield was even increased to 50% with 55% conversion after stirring for 20 h. Similarly, applying the urea- H_2O_2 adduct improved results were obtained with ligand **2**. Hence, we propose that ligand **12** favor the production of inactive μ -oxo complexes (Fig. 5, proposed and observed in [15b]), more than ligand **2**, which is consistent with the obtained and catalytic active X-ray structures.

In the reaction with ligand **2**, 50% hydrogen peroxide and 10 equiv. of labeled water no incorporation of labeled oxygen into the epoxide (50% yield with 52% conversion) was noticed. Only traces of the side product benzaldehyde (~1% yield) showed incorporation of ^{18}O in an amount of approximately 1/3. Hence, for this reaction the oxo-hydroxo tautomerism is to slow or no high-valent iron-oxo species does exist in our system. Furthermore, the role of air, which is known to support autooxidation processes in many non-heme model systems was examined [27]. Thus, the model epoxidation reaction was performed under inert conditions. In the presence of ligand **2** no variation of yield was obtained compared to the epoxidation on air. These findings demonstrate the stability of our catalyst system which works smoothly in the presence of air and suppresses autooxidation processes, which is different from most non-heme model systems.

While studying the effects of different ligands, a novel crystal structure was obtained directly from the reaction mixture of

our applied epoxidation system (Fig. 5c). In addition to the μ -oxo-diiron complexes (Fig. 5b) and the mononuclear iron complexes with four imidazole ligands (Fig. 5d), we were able to discover a neutral iron complex consisting of three imidazole ligands and three chloride ions. Fig. 5 shows the structurally different complexes found in our reaction system.

The novel octahedral *mer*-[Fe^{III}(**13**)Cl₃] complex is structurally similar to *mer*-[Fe(*N*-methylimidazole)₃Cl₃] reported by Cotton et al. [28]. However, the iron chloride distances in *mer*-[Fe^{III}(**13**)Cl₃] *trans*- to nitrogen(N3) (Fe-Cl2 = 2.3096(5) Å) and *trans*- to Cl1 (Fe-Cl3 = 2.3071(6) Å) are significantly shorter than the Fe-Cl1 distance with 2.3777(6) Å. Compared to *trans*-[FeCl₂(**2**)₄]Cl with distances (Fe-Cl1 = 2.3115(6) Å) and (Fe-Cl2 = 2.3036(7) Å) the long Fe-Cl1 distance in *mer*-[Fe^{III}(**13**)Cl₃] is also unexpected. Probably, this is a hint for a facilitated exchange with an imidazole ligand to give the other catalytically active *trans*-[FeCl₂(imidazole)₄]Cl species. To prove these findings we tested the molecular-defined complexes under our reaction conditions. The found catalytic reactivity is consistent with our assumption (Scheme 3).

Although the complex is structurally different from *trans*-[FeCl₂(**2**)₄]Cl, it is clearly shown that the novel mononuclear iron complex [FeCl₃(**13**)₃] is an active, highly selective and defined epoxidation catalyst.

4. Conclusion

The iron/imidazole catalyst system allows for a biomimetic and convenient epoxidation of various aromatic and aliphatic olefins using environmentally benign hydrogen peroxide as oxidant. Both the in situ catalysts as well as the molecular-defined iron species are cheap and easy-to-use without any special precautions. With respect to the mechanism of this reaction important insights have been obtained. While most of the known non-heme iron-based epoxidation systems require oxygen free atmosphere, the stability towards air and water of our system is remarkable. Notably, both the ligand and the used substrate show a strong influence on the reactivity and the different reaction pathways. It is shown that modification of the ligand structure alters also the structure of the resulting mono- or binuclear iron complexes. It is likely, that under reaction conditions there is equilibrium between the different characterized complexes.

Acknowledgements

We thank the State of Mecklenburg-Western Pomerania, the Federal Ministry of Education and Research (BMBF) and the Deutsche Forschungsgemeinschaft (SPP 1118 and Leibniz-prize) for financial support. K. Schröder appreciates the financial support provided by the Graduiertenkolleg 1213 "Neue Methoden für Nachhaltigkeit in Katalyse und Technik" and the Max-Buchner-

Forschungsstiftung (DECHEMA). Dr. habil. M. K. Tse and Dr. B. Join are acknowledged for fruitful discussions and M. Heyken for technical assistance.

References

- [1] H. Orzesek, R.P. Schulz, U. Dingerdissen, W.F. Maier, *Chem. Eng. Technol.* 22 (1999) 691.
- [2] (a) M.G. Clerici, G. Bellussi, U. Romano, *J. Catal.* 129 (1991) 159; (b) R. Murugavel, H.W. Roesky, *Angew. Chem. Int. Ed.* 36 (1997) 477.
- [3] S. Linic, H. Piao, K. Adib, M.A. Barteau, *Angew. Chem. Int. Ed.* 43 (2004) 2918.
- [4] For excellent mechanistic investigations in heterogeneous catalysis, see: G. Ertl, H. Knözinger, F. Schüth, J. Weitkamp, *Handbook of Heterogeneous Catalysis*, second ed., Wiley-VCH, Weinheim, 2008.
- [5] M.K. Tse, C. Döbler, S. Bhor, M. Klawonn, W. Mägerlein, H. Hugl, M. Beller, *Angew. Chem. Int. Ed.* 43 (2004) 5255.
- [6] W.A. Herrmann, R.W. Fischer, D.W. Marz, *Angew. Chem. Int. Ed.* 30 (1991) 1638.
- [7] E.M. McGarrigle, D.G. Gilheany, *Chem. Rev.* 105 (2005) 1563.
- [8] (a) A. Correa, O. García Mancheño, C. Bolm, *Chem. Soc. Rev.* 37 (2008) 1108; (b) B.S. Lane, K. Burgess, *Chem. Rev.* 103 (2003) 2457.
- [9] S. Enthaler, K. Junge, M. Beller, *Angew. Chem. Int. Ed.* 47 (2008) 3317.
- [10] M. Merckx, D.A. Kopp, M.H. Sazinsky, J.L. Blazyk, J. Müller, S.J. Lippard, *Angew. Chem. Int. Ed.* 40 (2001) 2782.
- [11] For a list of common oxidants, their active oxygen contents and waste products, see: J.-E. Bäckvall, *Modern Oxidation Methods*, Wiley-VCH, Weinheim, 2004, p. 22.
- [12] For the epoxidation of aromatic olefins see: (a) B. Bitterlich, G. Anilkumar, F.G. Gelalcha, B. Spilker, A. Grotevendt, R. Jackstell, M.K. Tse, M. Beller, *Chem. Asian J.* 2 (2007) 521; (b) F.G. Gelalcha, B. Bitterlich, G. Anilkumar, M.K. Tse, M. Beller, *Angew. Chem. Int. Ed.* 46 (2007) 7293.
- [13] For the epoxidation of aliphatic olefins see: B. Bitterlich, K. Schröder, M.K. Tse, M. Beller, *Eur. J. Org. Chem.*, 29 (2008) 4867.
- [14] (a) K. Schröder, S. Enthaler, B. Join, K. Junge, M. Beller, *Adv. Synth. Catal.* 352 (2010), accepted for publication; (b) S. Enthaler, K. Schröder, S. Inuo, B. Eckhardt, K. Junge, M. Beller, M. Driess, *Eur. J. Org. Chem.*, submitted for publication.
- [15] (a) K. Schröder, X. Tong, B. Bitterlich, M.K. Tse, F.G. Gelalcha, A. Brückner, M. Beller, *Tetrahedron Lett.* 48 (2007) 6339; (b) K. Schröder, S. Enthaler, B. Bitterlich, T. Schulz, A. Spannenberg, M.K. Tse, K. Junge, M. Beller, *Chem. Eur. J.* 15 (2009) 5471.
- [16] (a) S. Fujii, Y. Maki, H. Kimoto, *J. Fluorine Chem.* 43 (1989) 131; (b) B.E. Ketz, A.P. Cole, R.M. Waymouth, *Organometallics* 23 (2004) 2835, references cited herein.
- [17] G.M. Sheldrick, *Acta Crystallogr. A* 64 (2008) 112.
- [18] A.L. Spek, PLATON, A Multipurpose Crystallographic Tool, Utrecht University, Utrecht, The Netherlands, 2005.
- [19] L. Que Jr., W.B. Tolman, *Nature* 455 (2008) 333.
- [20] (a) A. Karlsson, J.V. Parales, R.E. Parales, D.T. Gibson, H. Eklund, S. Ramaswamy, *Science* 299 (2003) 103; (b) PDB ID:1o7g; Data were taken from Research Collaboratory for Structural Bioinformatics PDB (<http://www.pdb.org/>) and arranged with MBT Protein workshop (J.L. Moreland, A. Gramada, O.V. Buzko, Q. Zhang, P.E. Bourne, *BMC Bioinformatics* (2005) 6).
- [21] Examples for the incorporation of oxygen to iron(II) complexes to form μ -oxoiron(III) derivatives: (a) A. Machkour, D. Mandon, M. Lachkar, R. Welter, *Inorg. Chem.* 43 (2004) 1545; (b) N.K. Thallaj, O. Rotthaus, L. Benhamou, N. Humbert, M. Elhabiri, M. Lachkar, R. Welter, A.-M. Albrecht-Gary, D. Mandon, *Chem. Eur. J.* 14 (2008) 6742.
- [22] F. Bellesia, L. Forti, F. Gheli, U.M. Pagnoni, *Synth. Commun.* 27 (1997) 961.
- [23] For an example with a semiquinone as ligand, see: M.E. Bodini, P.E. Bravo, V. Arancibia, *Polyhedron* 13 (1994) 497.
- [24] S. Noda, K. Sanehira, T. Doba, H. Yoshida, *Bull. Chem. Soc. Jpn.* 55 (1982) 1705.
- [25] R.A. Sheldon, I.W.C.E. Arends, *Adv. Synth. Catal.* 346 (2004) 1051.
- [26] (a) A. Company, L. Gómez, X. Fontrodona, X. Ribas, M. Costas, *Chem. Eur. J.* 14 (2008) 5727; (b) J. Bautz, P. Comba, C. Lopez de Laorden, M. Menzel, G. Rajaraman, *Angew. Chem. Int. Ed.* 46 (2007) 8067.
- [27] A. Company, Y. Feng, M. Güell, X. Ribas, J.M. Luis, L. Que Jr., M. Costas, *Chem. Eur. J.* 15 (2009) 3359.
- [28] S.A. Cotton, V. Franckevicius, F. Fawcett, *Polyhedron* 21 (2002) 2055.